arXiv:1510.06924v1 [hep-ph] 23 Oct 2015

The longitudinal and transverse distributions of the pion wavefunction from the present experimental data on the pion-photon transition form factor

Tao Zhong[1],* Xing-Gang Wu[2],† and Tao Huang[3]‡
[1] *Department of Physics, Henan Normal University, Xinxiang 453007, P.R. China*
[2] *Department of Physics, Chongqing University, Chongqing 401331, P.R. China*
[3] *Institute of High Energy Physics and Theoretical Physics Center for Science Facilities, Chinese Academy of Sciences, Beijing 100049, P.R. China*

(Dated: October 26, 2015)

It is noted that the low-energy behavior of the pion-photon transition form factor $F_{\pi\gamma}(Q^2)$ is sensitive to the transverse distribution of the pion wavefunction, and its high-energy behavior is sensitive to the longitudinal one. Thus a careful study on $F_{\pi\gamma}(Q^2)$ can provide helpful information on the pion wavefunction precisely. In this paper, we present a combined analysis of the data on $F_{\pi\gamma}(Q^2)$ reported by the CELLO, the CLEO, the BABAR and the BELLE collaborations. It is performed by using the method of least squares. By using the combined measurements of BELLE and CLEO Collaborations, the pion wavefunction longitudinal and transverse behavior can be fixed to a certain degree, i.e. we obtain $\beta \in [0.691, 0.757]$GeV and $B \in [0.00, 0.235]$ for $P_{\chi^2} \geq 90\%$, where β and B are two parameters of a convenient pion wavefunction model whose distribution amplitude can mimic the various longitudinal behavior under proper choice of parameters. We observe that the CELLO, CLEO and BELLE data are consistent with each other, all of which prefers the asymptotic-like distribution amplitude; while the BABAR data prefers a more broad distribution amplitude, such as the CZ-like one.

PACS numbers: 12.38.-t, 12.38.Bx, 14.40.Aq

I. INTRODUCTION

The pion-photon transition form factor (TFF) $F_{\pi\gamma}(Q^2)$ provides a simplest example for the perturbative QCD (pQCD) application to exclusive processes, where Q^2 stands for the momentum transfer. The TFF relates two photons with the lightest meson (pion) and provides a good platform for studying longitudinal and transverse properties of the pion wavefunction.

The pion-photon TFF $F_{\pi\gamma}(Q^2)$ can be measured via the process, $e^+e^- \to e^+e^-\pi^0$, in a single-tagged mode. It was first measured in a low-energy region $Q^2 < 3\text{GeV}^2$ by the CELLO collaboration [1]. Later on, it was measured by the CLEO collaboration [2] in the energy region $Q^2 \in [1.5, 9.2]\text{GeV}^2$, and by the BABAR collaboration [3] and the BELLE collaboration [4] in the widest energy region $Q^2 \in [4, 40]\text{GeV}^2$. On the other hand, it has been theoretically predicted by using the pQCD approach, the QCD light-cone sum rules, or some phenomenological models such as the semi-bosonized Nambu-Jona-Lasinio model and the nonlocal chiral-quark model [5–20]. For example, Lepage and Brodsky studied the pion-photon TFF by neglecting the transverse distributions ($\mathbf{k}_\perp$-distribution) of the constitute quarks, and resulted in the well-known asymptotic prediction [5], i.e., $Q^2F_{\pi\gamma}(Q^2)$ tends to be a constant ($\sqrt{2}f_\pi$) for the asymptotic pion DA $\phi_\pi^{\rm as}(x,Q^2)|_{Q^2\to\infty} = 6x(1-x)$. The pion decay constant $f_\pi = 130.41 \pm 0.03 \pm 0.20$MeV [21].

When $Q^2 \sim$ a few GeV^2, one should take into account the $\mathbf{k}_\perp$-corrections such that to achieve a reliable prediction of $F_{\pi\gamma}(Q^2)$ [6–12]. The experimental data in this Q^2-region is then helpful for determining the transverse behavior of the pion wavefunction. When Q^2 is large enough, the $\mathbf{k}_\perp$-terms become less important, and the pion-photon TFF shall be dominated by the longitudinal behavior of the pion wavefunction,which is related to the pion distribution amplitude (DA). At present, there is no definite conclusion on the pion DA due to the dramatic difference between the BABAR and BELLE data. The experimental data in the large Q^2-region is thus helpful for determining the longitudinal behavior of the pion wavefunction.

In the paper, we shall study the pion-photon TFF $F_{\pi\gamma}(Q^2)$ by using a convenient pion wavefunction constructed from the revised light-cone harmonic oscillator model, whose DA can conveniently mimic the Asymptotic-like to more broad longitudinal behavior via proper choices of input parameters. Then we perform a combined analysis of the experimental data reported by the CELLO, the CLEO, the BABAR and the BELLE collaborations, with an attempt to extract useful information of the pion wavefunction. For the purpose, we shall adopt the analytical expression of $F_{\pi\gamma}(Q^2)$ suggested in our previous paper [13] as its basic fitting function. The pion wavefunction parameters shall then be fitted by comparing the experimental data with the help of the method of least squares such that to achieve the best goodness-of-fit.

The remaining parts of the paper are organized as follows. In Sec.II, we give a short review on the pion-photon TFF $F_{\pi\gamma}(Q^2)$ and a brief introduction of the method of least squares. A combined analysis for the experimental

*Electronic address: zhongtao@htu.edu.cn
†Electronic address: wuxg@cqu.edu.cn
‡Electronic address: huangtao@ihep.ac.cn

data reported by the CELLO, the CLEO, the BABAR and the BELLE collaborations is presented in Sec.III. In Sec.IV, we analyze the TFF $F_{\pi\gamma}(Q^2)$ in detail by using the BELLE and the CLEO data as an attempt to find more accurate information on the pion wavefunction. Sec.V is reserved for a summary.

II. A BRIEF REVIEW OF THE PION-PHOTON TFF AND THE METHOD OF LEAST SQUARES

The pion-photon TFF can be divided into two parts

$$F_{\pi\gamma}(Q^2) = F_{\pi\gamma}^{(V)}(Q^2) + F_{\pi\gamma}^{(NV)}(Q^2). \tag{1}$$

$F_{\pi\gamma}^{(V)}(Q^2)$ stands for the contribution from the valence-quark part, which is pQCD calculable. The analytical expression of $F_{\pi\gamma}^{(V)}(Q^2)$ can be found in Ref.[13], in which the next-to-leading order contributions [22–24] and the $\mathbf{k}_\perp$-dependence has been kept explicitly, i.e.

$$F_{\pi\gamma}^{(V)}(Q^2) = \frac{1}{4\sqrt{3}\pi^2}\int_0^1\int_0^{x^2Q^2}\frac{dx}{xQ^2}\left[1-\frac{C_F\alpha_s(Q^2)}{4\pi}\left(\ln\frac{\mu_f^2}{xQ^2+k_\perp^2}+2\ln x+3-\frac{\pi^2}{3}\right)\right]\cdot\Psi_{q\bar{q}}(x,k_\perp^2)dk_\perp^2, \tag{2}$$

where $[dx]=dxdx'\delta(1-x-x')$, $C_F=4/3$ and $k_\perp=|\mathbf{k}_\perp|$. $\mu_f=Q$ stands for the factorization scale. $F_{\pi\gamma}^{(NV)}(Q^2)$ stands for the nonvalence-quark part contribution that is related to the higher Fock states of pion, which can be estimated via a proper phenomenological model [12],

$$F_{\pi\gamma}^{(NV)}(Q^2) = \frac{\alpha}{(1+Q^2/\kappa^2)^2}, \tag{3}$$

where $\kappa=\sqrt{-\frac{F_{\pi\gamma}(0)}{\frac{\partial}{\partial Q^2}F_{\pi\gamma}^{(NV)}(Q^2)|_{Q^2\to 0}}}$ and $\alpha=\frac{1}{2}F_{\pi\gamma}(0)$. It indicates $F_{\pi\gamma}^{(NV)}(Q^2)$ is $1/Q^2$-suppressed to $F_{\pi\gamma}^{(V)}(Q^2)$ in large Q^2-region, then it gives negligible contribution to the TFF at large Q^2-region.

The pion-photon TFF $F_{\pi\gamma}(Q^2)$ is a convolution of hard scattering amplitude with the $\mathbf{k}_\perp$-correction and the pion wavefunction. By taking the BHL-prescription [25], the pion wavefunction can be constructed over the light-cone harmonic oscillator model [13], i.e.

$$\Psi_{q\bar{q}}(x,\mathbf{k}_\perp) = \frac{m_q}{\sqrt{\mathbf{k}_\perp^2+m_q^2}}A\varphi(x)\exp\left[-\frac{\mathbf{k}_\perp^2+m_q^2}{8\beta^2x(1-x)}\right], \tag{4}$$

where m_q is the mass of constituent quark, A is the normalization constant, β is the harmonic parameter, and $\varphi(x)=1+B\times C_2^{3/2}(2x-1)$ dominates the longitudinal distribution with the Gegenbauer polynomial $C_2^{3/2}(2x-1)$. After integrating over the transverse momentum dependence, we obtain the pion DA

$$\phi_{q\bar{q}}(x,\mu_0^2) = \frac{\sqrt{3}Am_q\beta}{2\pi^{3/2}f_\pi}\sqrt{x(1-x)}\varphi(x)\times\left\{\mathrm{Erf}\left[\sqrt{\frac{m_q^2+\mu_0^2}{8\beta^2x(1-x)}}\right]-\mathrm{Erf}\left[\sqrt{\frac{m_q^2}{8\beta^2x(1-x)}}\right]\right\}, \tag{5}$$

where the initial scale $\mu_0\sim 1$ GeV, the error function $\mathrm{Erf}(x)=\frac{2}{\sqrt{\pi}}\int_0^x d^{-t^2}dt$. The pion DA satisfies the normalization condition, $\int_0^1 dx\phi_{q\bar{q}}(x,\mu_0^2)=1$. The input model parameters can be fitted from the known experimental data. In addition, one extra constraint from the sum rules of $\pi^0\to\gamma\gamma$ shall be adopted, which states $\int_0^1 dx\Psi_{q\bar{q}}(x,\mathbf{k}_\perp=0)=\frac{\sqrt{6}}{f_\pi}$. We can adopt this and the normalization condition to fix the values of A and β, leaving m_q and B as the two free parameters to be determined from the data. Ref.[13] has observed that if setting m_q to be the usually choosing 300 MeV, the pion DA (5) shall change from the asymptotic-like form [5] to the CZ-like form [26] by simply shifting the parameter B from 0.00 to 0.60. In the present paper, to be more general, we shall adopt a broader range $m_q\in[200,400]$MeV and $B\in[0.00,0.60]$ to do our fit.

The data fit shall be done by using the method of least squares. Considering a set of N independent measurements y_i with the known variance σ_i and the mean $\mu(x_i;\theta)$ at known points x_i. The measurements y_i are assumed to be in Gaussian distribution. The goal of the method of least squares is to get the preferable value of θ by minimizing the likelihood function [21]

$$\chi^2(\theta) = \sum_{i=1}^{N} \frac{(y_i - \mu(x_i,\theta))^2}{\sigma_i^2}. \tag{6}$$

As for the present case, the function $\mu(x_i;\theta)$ stands for the pion-photon TFF function defined by (1) and $\theta = (m_q, B)$; The value of y_i and its variance σ_i for the pion-photon TFF can be read from the measurements of the CELLO, the CLEO, the BABAR and the BELLE collaborations [1–4], respectively. The goodness-of-fit is judged by the magnitude of the probability

$$P_{\chi^2} = \int_{\chi^2}^{\infty} f(y;n_d)dy, \tag{7}$$

where $f(y;n_d) = \frac{1}{\Gamma(\frac{n_d}{2})2^{n_d/2}} y^{\frac{n_d}{2}-1}e^{-\frac{y}{2}}$ is the probability density function of χ^2, and n_d is the number of degree-of-freedom. The probability P_{χ^2} is within the range of $[0,1]$; when its value is closer to 1, a better fit is assumed to be achieved.

III. BEST FIT OF THE CELLO, THE CLEO, THE BABAR AND THE BELLE DATA ON $F_{\pi\gamma}(Q^2)$

	CELLO	CLEO	BABAR	BELLE
m_q(MeV)	216	246	347	222
B	0.000	0.002	0.600	0.000
A(GeV^{-1})	20.695	21.823	19.438	20.906
β(GeV)	0.801	0.697	0.664	0.776
$\chi^2_{\rm min}/n_d$	4.795/3	4.380/13	15.508/15	5.657/13
$P_{\chi^2_{\rm min}}$	0.187	0.986	0.416	0.958

TABLE I: The wavefunction parameters which are fixed by using the method of least squares for the CELLO, the CLEO, the BABAR and the BELLE data, respectively.

We adopt Eq.(1) as the basic input function to achieve a best fit of the pion wavefunction parameters by using the known experimental data on the TFF $F_{\pi\gamma}(Q^2)$. More specifically, the values of the two free parameters (m_q, B) are fixed by requiring them to achieve the minimum value of $\chi^2(m_q, B)$, which indicates a best fit of the experimental data within the allowable parameter spaces. The determined pion wavefunction parameters for the data of the BABAR, the BELLE, the CLEO and the CELLO collaborations are presented in Table I, where the values of $\chi^2_{\rm min}/n_d$ and the probability $P_{\chi^2_{\rm min}}$ are also presented. The pion-photon TFFs under those parameters are put in Fig.(1). Fig.(1) shows that the BELLE, the

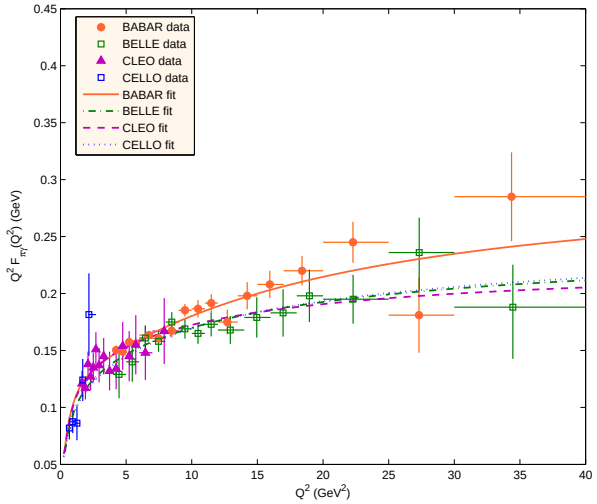

FIG. 1: The pion-photon TFFs $Q^2F_{\pi\gamma}(Q^2)$ for the experimental data measured by the BABAR, the BELLE, the CLEO and the CELLO Collaborations, respectively. The fitted curves are obtained by using the method of least squares.

CLEO and the CELLO data result in similar trend of the pion-photon TFF, while the BABAR data leads to a quite different TFF behavior in larger Q^2-region, i.e. $Q^2 > 10$ GeV^2.

Table I shows a better fit with better confidence level can be achieved from the CLEO and the BELLE data, whose probabilities are 0.986 and 0.958, respectively. The low probability of the CELLO data is reasonable due to small number of data. The probability of the BABAR data is less than 0.50, indicating there may have some questionable points. This conclusion agrees with the arguments of Refs.[16–19]. By using the EKHARA event generator [27], a Mont Carlo simulation of the pion-photon TFF on the BESIII platform within the energy region $Q^2 < 3.1$GeV^2 has been given in Ref.[28]. Those simulation data lead to: $m_q = 272$ MeV, $B = 0.058$, $A = 22.118$GeV^{-1}, $\beta = 0.656$ GeV, $\chi^2_{\rm min}/n_d = 4.521/16$ and $P_{\chi^2_{\rm min}} = 0.998$, which is also consistent with the above BELLE, CELLO and CLEO predictions.

IV. THE PION WAVEFUNCTION FROM THE BELLE AND THE CLEO DATA

In the above section, the pion wavefunction parameters are fixed by minimizing the likelihood function χ^2. In present section, we shall adopt a weaker constraint from the probability P_{χ^2} to do a more detailed discussion on possible constraints on the pion wavefunction. This is reasonable, since the present data themselves are of certain uncertainties and we do not need to require the theoretical prediction to fit the data extremely well. The future more precise data shall lead to more strict con-

straints. In this section, we shall only adopt the BELLE and CLEO data to do the discussion, since they are at the more confidence level.

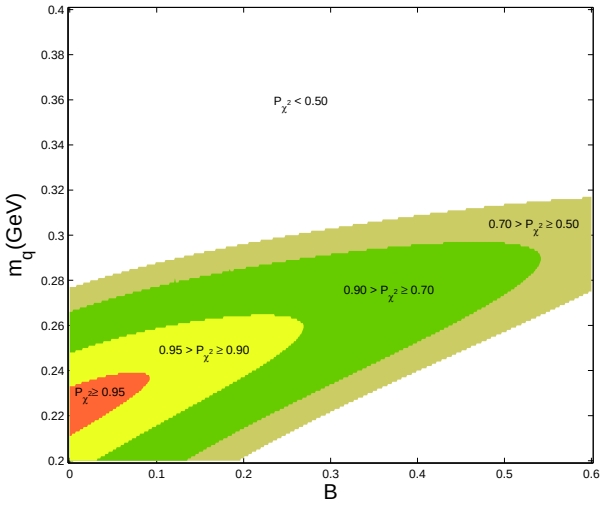

FIG. 2: The allowable (m_q, B)-region versus the probability P_{χ^2} from the BELLE data for $Q^2 \in [4, 40]\text{GeV}^2$. The four shaded bands from inside to outside are for $P_{\chi^2} \geq 95\%$, $90\% \leq P_{\chi^2} < 95\%$, $70\% \leq P_{\chi^2} < 90\%$ and $50\% \leq P_{\chi^2} < 70\%$, respectively.

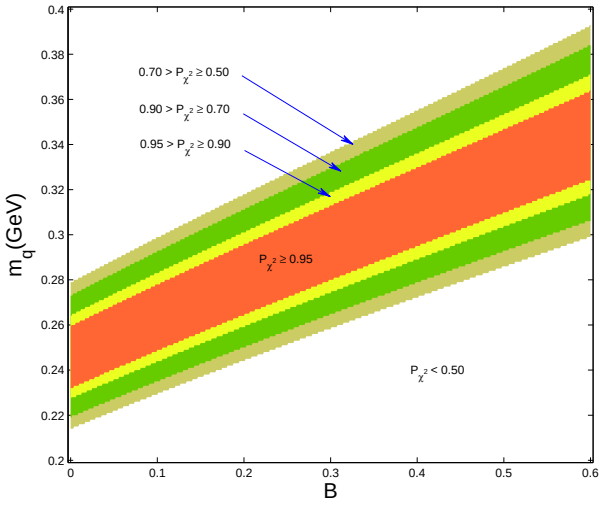

FIG. 3: The allowable (m_q, B)-region versus the probability P_{χ^2} from the CLEO data for $Q^2 \in [1.5, 9.2]\text{GeV}^2$. The four shaded bands from inside to outside are for $P_{\chi^2} \geq 95\%$, $90\% \leq P_{\chi^2} < 95\%$, $70\% \leq P_{\chi^2} < 90\%$ and $50\% \leq P_{\chi^2} < 70\%$, respectively.

Figs.(2,3) show the allowable (m_q, B)-region versus the probability P_{χ^2} from either the BELLE or CLEO data, where the four shaded bands from inside to outside are for $P_{\chi^2} \geq 95\%$, $90\% \leq P_{\chi^2} < 95\%$, $70\% \leq P_{\chi^2} < 90\%$ and $50\% \leq P_{\chi^2} < 70\%$, respectively. Figs.(2,3) show that a more strict constraint to the parameters can be achieved by a more bigger probability P_{χ^2}.

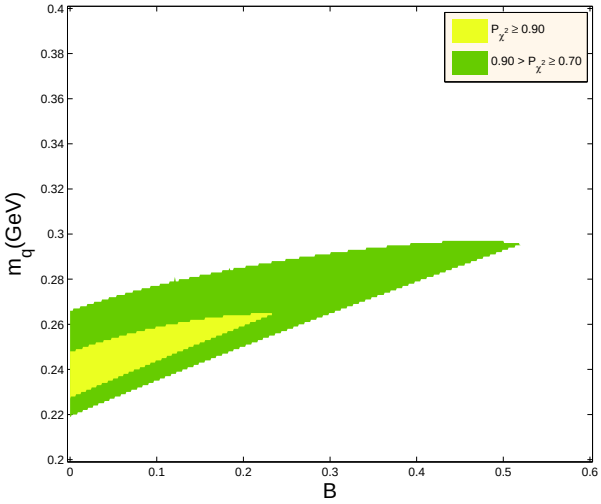

FIG. 4: The allowable (m_q, B)-region from both the BELLE and the CLEO data, where the light-color band is for $P_{\chi^2} \geq 90\%$ and the fuscous band is for $70\% \leq P_{\chi^2} < 90\%$.

As a combination, we put the allowable (m_q, B)-region from both the BELLE and CLEO data in Fig.(4). Fig.(4) shows that if requiring $P_{\chi^2} \geq 90\%$, we shall obtain $B \in [0, 0.235]$ and $m_q \in [227, 265]$MeV, which then lead to the range of the first two Gegenbauer moments of the pion DA: $a_2(1\text{GeV}) = [0.087, 0.348]$ and $a_4(1\text{GeV}) = [-0.007, 0.015]$. The predicted a_2 agrees with the ones determined in the literature from other approaches or other processes, i.e. $a_2(1\text{GeV}) = 0.26^{+0.21}_{-0.09}$ [29] and 0.19 ± 0.06 [30] by QCD sum rules on the pion-photon TFFs; $0.24 \pm 0.14 \pm 0.08$ [31], 0.20 ± 0.03 [32] and 0.19 ± 0.05 [33] by QCD LCSRs on the pion form factors; $0.19 \pm 0.19 \pm 0.08$ [34], $0.17^{+0.15}_{-0.17}$ [35] and 0.112 ± 0.073 [36] by LCSRs analysis on the $B/D \to \pi l \nu$.

It is noted that $a_2 \sim B$, indicating that the longitudinal behavior of the pion wavefunction is dominantly determined by the parameter B. The BELLE data provides a strong constraint for both B and m_q, especially for $P_{\chi^2} \geq 90\%$. On the other hand, Fig.(3) shows by using the lower Q^2-data alone, one cannot determine the pion wavefunction's longitudinal behavior, because in the low Q^2-region, the TFF is insensitive to the choice of the parameter B [1]. However as will be shown later, the low-energy data is helpful for determining the transverse

[1] For a bigger B, one only needs a reasonable bigger constitute quark mass m_q to get the same TFF. This observation agrees with the prediction of Ref.[12].

behavior of the pion wavefunction.

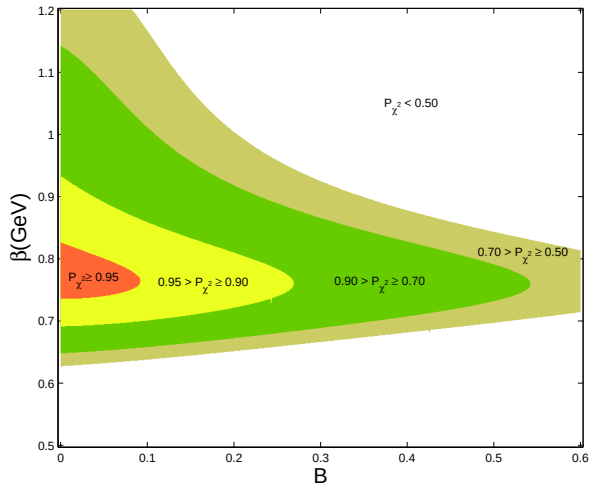

FIG. 5: The allowable (β, B)-region versus the probability P_{χ^2} from the BELLE data, where $Q^2 \in [4, 40]\text{GeV}^2$. The four shaded bands from inside to outside are for $P_{\chi^2} \geq 95\%$, $90\% \leq P_{\chi^2} < 95\%$, $70\% \leq P_{\chi^2} < 90\%$ and $50\% \leq P_{\chi^2} < 70\%$, respectively.

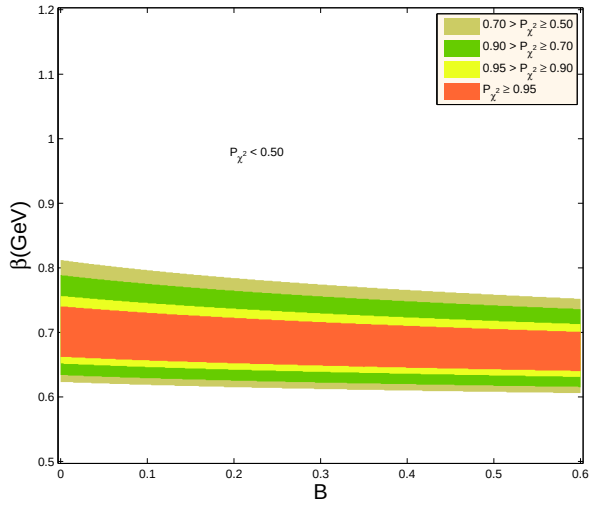

FIG. 6: The allowable (β, B)-region versus the probability P_{χ^2} from the CLEO data, where $Q^2 \in [1.5, 9.2]\text{GeV}^2$. The four shaded bands from inside to outside are for $P_{\chi^2} \geq 95\%$, $90\% \leq P_{\chi^2} < 95\%$, $70\% \leq P_{\chi^2} < 90\%$ and $50\% \leq P_{\chi^2} < 70\%$, respectively.

The transverse behavior of the pion wavefunction is dominated by the harmonic parameter β [37]. To show how the experimental data affect the transverse behavior, we take the parameters (B,β) as the two free input parameters. Following the same fit procedures, we can obtain the allowable ranges for the parameters (B,β). The results are presented in Figs.(5,6), which are for the BELLE and the CLEO data, respectively. Here the four shaded bands from inside to outside are for $P_{\chi^2} \geq 95\%$, $90\% \leq P_{\chi^2} < 95\%$, $70\% \leq P_{\chi^2} < 90\%$ and $50\% \leq P_{\chi^2} < 70\%$, respectively.

The BELLE data leads to $\beta \in [0.691, 0.933]$GeV and $B \in [0.00, 0.269]$ for $P_{\chi^2} \geq 90\%$. Fig.(5) shows the allowed β range shall be quickly expanded when P_{χ^2} becomes smaller. For example, when $B = 0.20$, we have $\beta \in [0.721, 0.810]$ for $P_{\chi^2} \geq 90\%$, $\beta \in [0.672, 0.918]$ for $P_{\chi^2} \geq 70\%$ and $\beta \in [0.651, 1.004]$ for $P_{\chi^2} \geq 50\%$. On the other hand, as shown by Fig.(6), the low-energy CLEO data can give a better constraint to the range of β, whose allowable range slightly increases with the decrement of P_{χ^2}. For example, we obtain $\beta \in [0.652, 0.757]$GeV for $P_{\chi^2} \geq 90\%$, $\beta \in [0.634, 0.789]$GeV for $P_{\chi^2} \geq 70\%$ and $\beta \in [0.623, 0.812]$GeV for $P_{\chi^2} \geq 50\%$, accordingly.

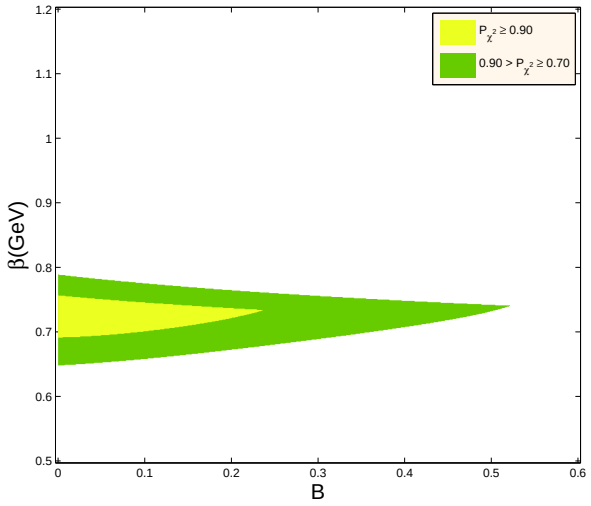

FIG. 7: The regions of the pion wavefunction parameters (β, B) from the BELLE and CLEO data under the probability $P_{\chi^2} \geq 90\%$, where the light-color band is for $P_{\chi^2} \geq 90\%$ and the fuscous band is for $70\% \leq P_{\chi^2} < 90\%$.

The allowable (β, B)-region from both the BELLE and CLEO data is presented in Fig.(7). The lower edge of the shaded band is determined by the BELLE data and the upper edge of the shaded band is determined by the CLEO data, which indicates that the low-energy data is important and helpful for determining the pion wavefunction's transverse behavior. Fig.(7) shows that $B \in [0.00, 0.235]$ and $\beta \in [0.691, 0.757]$GeV for $P_{\chi^2} \geq 90\%$.

The importance of the low-energy data can be further explained by Fig.(8), which shows the allowable (β, B)-region versus the probability P_{χ^2} from the BELLE data in high-energy region $Q^2 \in [10, 40]\text{GeV}^2$. Fig.(8) shows the allowable range of β is quickly broadened for a smaller and smaller P_{χ^2}. For example, when setting $B = 0.00$, we shall have $\beta \in [0.818, 0.887]$ for $P_{\chi^2} \geq 90\%$, $\beta \in [0.659, 1.111]$ for $P_{\chi^2} \geq 70\%$ and $\beta \in [0.613, 1.2]$ for

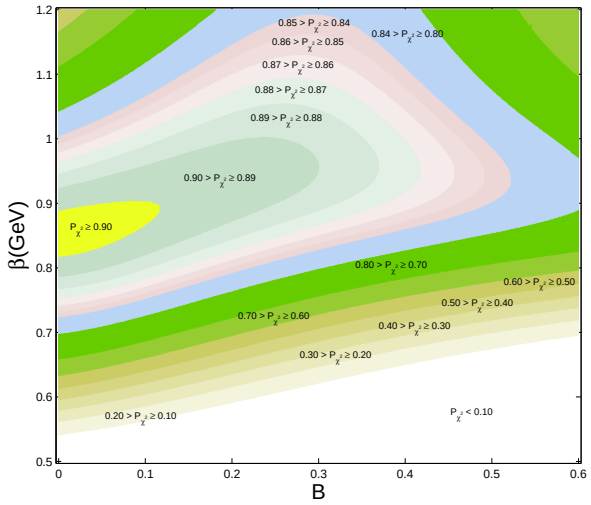

FIG. 8: The allowable (β, B)-region versus the choice of the probability P_{χ^2} from the BELLE data in the high-energy region $Q^2 \in [10, 40]\text{GeV}^2$.

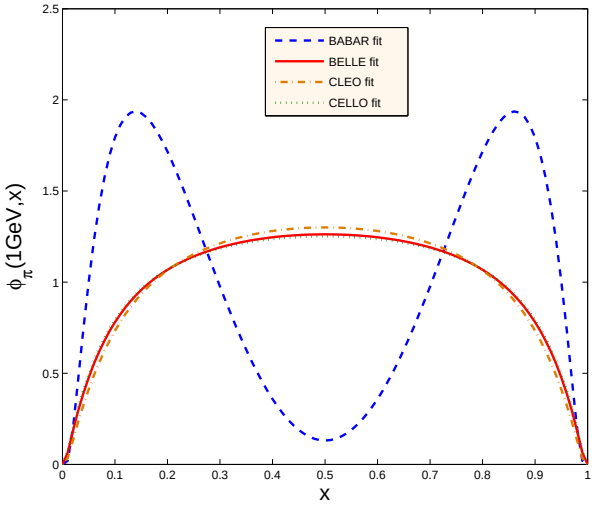

FIG. 9: The pion DAs with the parameters listed in Table I, which are fit from the TFF data of BABAR, BELLE, CLEO and CELLO collaborations, respectively.

$P_{\chi^2} \geq 50\%$. Thus by using the large Q^2 data alone, one may not get a definite conclusion on the transverse behavior, unless the goodness-of-fit is high enough.

V. SUMMARY

We have studied the transverse and longitudinal behavior of the pion wavefunction by fitting the CELLO, the CLEO, the BABAR and the BELLE data on the pion-photon TFF $F_{\pi\gamma}(Q^2)$. The method of least squares is adopted for such an analysis.

Using the best fit parameters that lead to minimized likelihood function, which are listed in Table I, we can get useful information on the pion wavefunction. As an example, we put its distribution amplitude in Fig.(9). It is shown that the best fit of the CELLO, the CLEO and the BELLE data prefer asymptotic-like behavior, while the BABAR data prefers the more broad distribution, such as the CZ-like behavior. Table I also indicates that a better fit with better confidence level can be achieved from the CLEO and the BELLE data, whose probabilities are close to 1. The low probability of the CELLO data is reasonable due to small number of data. The probability of the BABAR data is less than 0.50, indicating there may have some questionable points within the measured data.

The transverse and longitudinal behavior of the pion wavefunction is dominantly determined by the parameter β and B, respectively. The parameter B can be constrained by $Q^2F_{\pi\gamma}(Q^2)$ behaviors in high energy region precisely. For example, the BELLE data can determine the parameter B well. Figs.(3,6) show that if using the lower Q^2-data alone, such as the CLEO data, one cannot determine the pion wavefunction's longitudinal behavior. However, as shown by Fig.(6), the low-energy CLEO data is important and helpful for determining the transverse behavior of the pion wavefunction. However, one still cannot determine the pion wavefunction precisely due to the dramatic difference between the BABAR and BELLE data in the large Q^2-region. Therefore, the future experimental data in the large Q^2-region will be crucial for determining the longitudinal behavior of the pion wavefunction.

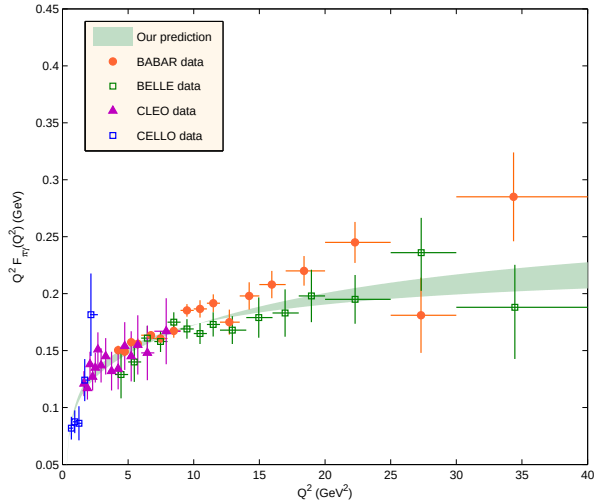

FIG. 10: The predicted pion-photon TFF $Q^2F_{\pi\gamma}(Q^2)$ by using the parameters determined from the BELLE and the CLEO data. The BABAR, the BELLE, the CLEO and the CELLO data are also presented as a comparison.

Using the BELLE and the CLEO data together and requiring $P_{\chi^2} \geq 90\%$, we obtain, $B \in [0, 0.235]$, $m_q \in [227, 265]$MeV and $\beta \in [0.691, 0.757]$GeV. Using those parameters, our final prediction on the pion-photon TFF $F_{\pi\gamma}(Q^2)$ are presented in Fig.(10).

Acknowledgments: This work was supported in part by the Natural Science Foundation of China under Grants No.11235005 and No.11275280, and by the Fundamental Research Funds for the Central Universities under Grant No.CDJZR305513.

[1] H. J. Behrend *et al.*, (CELLO Collaboration), Z. Phys. C **49**, 401 (1991).
[2] V. Savinov *et al.*,(CLEO Collaboration), arXiv:hep-ex/9707028; J. Gronberg *et al.*, (CLEO Collaboration), Phys. Rev. D **57**, 33 (1998).
[3] B. Aubert *et al.*, (BABAR Collaboration), Phys. Rev. D **80**, 052002 (2009).
[4] S. Uehara *et al.*, (Belle Collaboration), Phys. Rev. D **86**, 092007 (2012).
[5] G. P. Lepage and S. J. Brodsky, Phys. Rev. D **22**, 2157 (1980).
[6] F. G. Cao, T. Huang and B. Q. Ma, Phys. Rev. D **53**, 6582 (1996).
[7] R. Jakob *et al.*, J. Phys. G **22**, 45 (1996); P. Kroll and M. Raulfs, Phys. Lett. B **387**, 848 (1996); A. V. Radyushkin and R. Ruskov, Nucl. Phys. B **481**, 625 (1996).
[8] I. V. Musatov and A. V. Radyushkin, Phys. Rev. D **56**, 2713 (1997).
[9] N. G. Stefanis, W. Schroers and H. Ch. Kim, Eur. Phys. J. C **18**, 137 (2000).
[10] B. Melic, B.Nizic and K. Passek, Phys. Rev. D **65**, 053020 (2002).
[11] B. W. Xiao and B. Q. Ma, Phys. Rev. D **68**, 034020 (2003).
[12] T. Huang and X. G. Wu, Int. J. Mod. Phys. A **22**, 3065 (2007).
[13] X. G. Wu and T. Huang, Phys. Rev. D **82**, 034024 (2010).
[14] I. Balakireva, W. Lucha and D. Melikhov, PoS ConfinementX, 114 (2012); W. Lucha and D. Melikhov, PoS EPS-HEP **2013**, 445 (2013).
[15] X. G. Wu, T. Huang and T. Zhong, Chin. Phys. C **37**, 063105 (2013).
[16] A. P. Bakulev, S. V. Mikhailov, A. V. Pimikov and N. G. Stefanis, Phys. Rev. D **86**, 031501 (2012); A. V. Pimikov, A. P. Bakulev, S. V. Mikhailov and N. G. Stefanis, AIP Conf. Proc. **1492**, 134 (2012); N. G. Stefanis, A. P. Bakulev, S. V. Mikhailov and A. V. Pimikov, Phys. Rev. D **87** 094025 (2013).
[17] S. V. Mikhailov, A. V. Pimikov and N. G. Stefanis, Few Body Syst. **55**, 367 (2014).
[18] P. Kotko, Acta Phys. Polon. Supp. **6**, 195 (2013).
[19] D. Gómez Dumm, S. Noguera, N. N. Scoccola and S. Scopetta, Phys. Rev. D **89**, 054031 (2014).
[20] X. G. Wu and T. Huang, Chin. Sci. Bull. **59**, 3801 (2014).
[21] K. A. Olive, et al., (Particle Data Group), Chin. Phys. C **38**, 090001 (2014).
[22] I. V. Musatov and A. V. Radyushkin, Phys. Rev. D **56**, 2713 (1997).
[23] S. Nandi and H. N. Li, Phys. Rev. D **76**, 034008 (2007).
[24] H. N. Li and S. Mishima, Phys. Rev. D **80**, 074024 (2009).
[25] S. J. Brodsky, T. Huang, and G. P. Lepage, in *Particles and Fields-2*, Proceedings of the Banff Summer Institute, Ban8; Alberta, 1981, edited by A. Z. Capri and A. N. Kamal
(Plenum, New York, 1983), p. 143; G. P. Lepage, S. J. Brodsky, T. Huang, and P. B.Mackenize, *ibid.* , p. 83; T. Huang, in *Proceedings ofXXth International Conference on High Energy Physics*, Madison, Wisconsin, 1980, edited by L. Durand and L. G Pondrom, AIP Conf. Proc. No. 69 (AIP, New York, 1981), p. 1000.
[26] V. L. Chernyak and A. R. Zhitnitsky, Nucl. Phys. B **201**, 492 (1982).
[27] H. Czyz, S. Ivashyn, A. Korchin and O. Shekhovtsova, Phys. Rev. D **85**, 094010 (2012).
[28] A. Denig, arXiv:1412.2951.
[29] A. Khodjamirian, Th. Mannel and M. Melcher, Phys. Rev. D
70, 094002 (2004).
[30] A. P. Bakulev and S. V. Mikhailov, Phys. Lett. B **436**, 351 (1998); A. P. Bakulev, S. V. Mikhailov and N. G. Stefanis, Phys. Lett. B **508**, 279 (2001).
[31] V. M. Braun, A. Khodjamirian and M. Maul, Phys. Rev. D
61, 073004 (2000); J. Bijnens and A. Khodjamirian, Eur. Phys.
J. C **26**, 67 (2002).
[32] S. S. Agaev, Phys. Rev. D **72**, 074020 (2005).
[33] A. Schmedding and O. I. Yakovlev, Phys. Rev. D **62**, 116002 (2000).
[34] P. Ball and R. Zwicky, Phys. Lett. B **625**, 225 (2005).
[35] S. S. Agaev, Phys. Rev. D **72**, 114010 (2005);
73, 059902(E) (2006).
[36] T. Huang, T. Zhong and X. G. Wu, Phys. Rev. D **88**, 034013 (2013).
[37] T. Huang, B. Q. Ma and Q. X. Shen, Phys. Rev. D **49**, 1490 (1994).